

BAR EVOLUTION OVER THE LAST EIGHT BILLION YEARS: A CONSTANT FRACTION OF STRONG BARS IN GEMS

SHARDHA JOGEE¹, FABIO D. BARAZZA¹, HANS-WALTER RIX², ISAAC SHLOSMA³, MARCO BARDEN², CHRISTIAN WOLF⁴, JAMES DAVIES¹, INGE HEYER¹, STEVEN V.W. BECKWITH^{1,5}, ERIC F. BELL², ANDREA BORCH², JOHN A. R. CALDWELL¹, CHRISTOPHER J. CONSELICE⁶, TOMAS DAHLEN¹, BORIS HÄUSSLER², CATHERINE HEYMANS², KNUD JAHNKE⁷, JOHAN H. KNAPEN⁸, SEPPO LAINE⁹, GABRIEL M. LUBELL¹⁰, BAHRAM MOBASHER¹, DANIEL H. MCINTOSH¹¹, KLAUS MEISENHEIMER², CHIEN Y. PENG¹², SWARA RAVINDRANATH¹, SEBASTIAN F. SANCHEZ⁷, RACHEL S. SOMERVILLE¹ AND LUTZ WISOTZKI⁷
Accepted by ApJ Letters. To appear in Nov 2004 issue

ABSTRACT

One third of present-day spirals host optically visible strong bars that drive their dynamical evolution. However, the fundamental question of how bars evolve over cosmological times has yet to be resolved, and even the frequency of bars at intermediate redshifts remains controversial. We investigate the frequency of bars out to $z \sim 1$ drawing on a sample of 1590 galaxies from the Galaxy Evolution from Morphology and SEDs survey, which provides morphologies from *Hubble Space Telescope* Advanced Camera for Surveys (ACS) two-band images and accurate redshifts from the COMBO-17 survey. We identify spiral galaxies using three independent techniques based on the Sersic index, concentration parameter, and rest-frame color. We characterize bar and disk features by fitting ellipses to F606W and F850LP images, using the two bands to minimize shifts in the rest-frame bandpass. We exclude highly inclined ($i > 60^\circ$) galaxies to ensure reliable morphological classifications and apply different completeness cuts of $M_V \leq -19.3$ and -20.6 . More than 40% of the bars that we detect have semi major axes $a < 0''.5$ and would be easily missed in earlier surveys without the small point spread function of ACS. The bars that we can reliably detect are fairly strong (with ellipticities $e \geq 0.4$) and have a in the range ~ 1.2 – 13 kpc. We find that the optical fraction of such strong bars remains at $\sim 30\% \pm 6\%$ from the present-day out to look-back times of 2–6 Gyr ($z \sim 0.2$ – 0.7) and 6–8 Gyr ($z \sim 0.7$ – 1.0); it certainly shows no sign of a drastic decline at $z > 0.7$. Our findings of a large and similar bar fraction at these three epochs favor scenarios in which cold gravitationally unstable disks are already in place by $z \sim 1$ and where on average bars have a long lifetime (well in excess of 2 Gyr). The distributions of structural bar properties in the two slices are, however, not statistically identical and therefore allow for the possibility that the bar strengths and sizes may evolve over time.

Subject headings: galaxies: evolution — galaxies: general — galaxies: spiral — galaxies: structure

1. INTRODUCTION

It is widely recognized that stellar bars, either spontaneously or tidally induced, redistribute mass and angular momentum and thereby drive the dynamical and secular evolution of galaxies (e.g., Kormendy 1982; Shlosman, Frank, & Begelman 1989; Pfenniger & Norman 1990; Friedli & Benz 1993; Kormendy & Kennicutt 2004). In the local universe, one-third of local spiral galaxies host optically visible strong bars (e.g., Eskridge et al. 2002, hereafter E02; see also § 3). Mounting evidence, including observations of central molecular gas concentrations (e.g., Sakamoto et al. 1999), velocity fields (e.g., Regan, Vo-

gel, & Teuben 1997), and starbursts (e.g., Hunt & Malkan 1999; Jogee, Scoville, & Kenney 2004a), suggests that bars strongly influence their host galaxies. However, the most fundamental issues have yet to be resolved. When and how did bars form? Are bars a recent phenomenon or were they abundant at early cosmic epochs? Are bars long-lived or do they recurrently dissolve and re-form over a Hubble time? How do stellar bars fit within the hierarchical clustering framework of galaxy evolution and relate to the underlying disk evolution?

The evolution of a bar over a Hubble time depends on the host galaxy structure, the dark matter (DM) halo, and the environment. Numerical simulations of this complex

¹ Space Telescope Science Institute, 3700 San Martin Dr., Baltimore, MD 21218; jogee@stsci.edu

² Max-Planck Institute for Astronomy, Königstuhl 17, D-69117 Heidelberg, Germany

³ Department of Physics and Astronomy, University of Kentucky, Lexington, KY 40506-0055

⁴ Astrophysics, University of Oxford, Keble Road, Oxford OX1 3RH, U.K.

⁵ Department of Physics and Astronomy, Johns Hopkins University, Charles and 4th Street, Baltimore, MD 21218

⁶ Department of Astronomy, California Institute of Technology, Pasadena, CA 91125

⁷ Astrophysikalisches Institut Potsdam, An der Sternwarte 16, D-14482 Potsdam, Germany

⁸ Department of Physical Sciences, University of Hertfordshire, Hatfield, Herts AL10 9AB, U.K.

⁹ *Spitzer* Science Center, California Institute of Technology, Mail Code 220-6, 1200 East California Boulevard, Pasadena, CA 91125, U.S.A.

¹⁰ Department of Physics and Astronomy, Vassar College, Poughkeepsie, NY 12604, U.S.A.

¹¹ Department of Astronomy, University of Massachusetts, Amherst, MA 01003, U.S.A.

¹² Department of Astronomy, University of Arizona, 933 North Cherry Avenue, Tucson, AZ 85721, U.S.A.

process make widely different predictions (e.g., Friedli & Benz 1993; Shlosman & Noguchi 1993; El-Zant & Shlosman 2002; Athanassoula 2002; Bournaud & Combes 2002; Shen & Sellwood 2004), while the handful of observational results on bars at intermediate redshifts are conflicting. On the basis of 46 moderately inclined galaxies imaged with the Wide Field Planetary Camera2 (WFPC2) in the Hubble Deep Field (HDF), Abraham et al. (1999, hereafter A99) claim a dramatic decline in the rest-frame optical bar fraction (f_{opt}) from $\sim 24\%$ at $z \sim 0.2$ – 0.7 to below 5% at $z > 0.7$. On the basis of Near-Infrared Camera and Multi-Object Spectrometer (NICMOS) images of 95 galaxies in the HDF at $z \sim 0.7$ – 1.1 , Sheth et al. (2003, hereafter S03) detect four large bars with mean semi major axes a of 12 kpc ($1''.4$), while smaller bars presumably escaped detection because of the large NICMOS point spread function (PSF). S03 point out that their observed bar fraction of $\sim 5\%$ for large (12 kpc) bars at $z > 0.7$ is at least comparable to the local fraction of similarly large bars. From a study based on *HubbleSpaceTelescope* (*HST*) Advanced Camera for Surveys (ACS) F814W images of 186 galaxies over a 3.9×4.2 area in the Tadpole field, Elmegreen, Elmegreen, & Hirst (2004, hereafter E04) report a constant optical bar fraction of $\sim 20\%$ – 40% at $z \sim 0$ – 1.1 . This study is limited by the large (0.1–0.4) errors of the photometric redshifts (Benítez et al. 2004), and the small sample size precludes absolute magnitude completeness cuts. Furthermore, with only a single ACS filter, the rest-frame bandpass of the observations shifts by more than a factor of 2 over $z \sim 0$ – 1.1 .

In this Letter (see also Jogee et al. 2004b), we present the first results of an extensive study of bars at $z \sim 0.2$ – 1.0 , based on two-band ACS images covering $14' \times 14'$ ($\sim 25\%$) of the Galaxy Evolution from Morphology and SEDs (GEMS) survey. The area and the sample size of 1590 galaxies provide at least an order of magnitude better number statistics than earlier studies. We quantitatively identify bars using ellipse fits and minimize the effects of bandpass shifts by using both F850LP and F606W images (§ 2.2). Using highly accurate redshifts (§ 2.1), we compare the bar fractions in two redshift slices after applying completeness criteria. We show that the optical fraction of strong (ellipticities $e \geq 0.4$) bars is remarkably constant ($\sim 30\%$) from the present-day out to look-back times (T_{back}) of 2–6 Gyr ($z \sim 0.2$ – 0.7)¹³ and 6–8 Gyr ($z \sim 0.7$ – 1.0).

2. OBSERVATIONS, SAMPLE, AND METHODOLOGY

2.1. Observations and Sample Selection

GEMS is a two-band (F606W and F850LP) *HST* ACS imaging survey (Rix et al. 2004) of an 800 arcmin^2 ($\sim 28' \times 28'$) field centered on the Chandra Deep Field-South. GEMS consists of 78 one-orbit-long ACS pointings in each filter and reaches a limiting 5σ depth for point sources of 28.3 and 27.1 AB mag in F606W and F850LP, respectively. GEMS provides high-resolution ($\sim 0''.5$ or 360 pc at $z \sim 0.7$) ACS images for ~ 8300 galaxies in the redshift range $z \sim 0.2$ – 1.1 , where accurate redshifts [$\delta_z/(1+z) \sim 0.02$ down to $R_{\text{vega}} = 24$] and spectral energy distributions (SEDs) based on 17 filters exist from the COMBO-17 project (Wolf et al. 2004). For this Letter, we analyze only $\sim 25\%$ of the GEMS field as this area ($14' \times 14'$) is

already 30 times that of the HDF and yields good number statistics and robust results on the bar fraction (§ 3). It provides a sample that consists of 1590 galaxies in the range $z \sim 0.2$ – 1.0 and $R_{\text{vega}} \leq 24$. In a future paper (S. Jogee et al. in preparation, hereafter Paper II), we will use the entire GEMS sample to compare how bar properties evolve over 8 Gyr at 1 Gyr intervals.

2.2. Characterizing bars and f_{opt} out to $z \sim 1.0$

Table 1 illustrates the two methods that we use for assessing bar properties in two redshift slices at $0.25 < z \leq 0.70$ and $0.7 < z \leq 1.0$. The first method (referred to as Method I in Table 1) is to identify bars in the reddest filter (F850LP) at all z in order to minimize extinction and better trace old stars. However, with this method, the rest-frame bandpass shifts significantly, from I to B across the redshift range 0.2 – 1.0 . The second complementary method is to trace bars in both F606W and F850LP images such that the rest-frame band remains relatively constant, between B and V , out to $z \sim 1.0$.

We identify bars and other galactic components in F606W and F850LP images via the widely used (e.g., Wozniak et al. 1995; Jogee et al. 1999, 2002; Knapen et al. 2000) procedure of fitting ellipses using the standard IRAF “ellipse” routine. We developed a wrapper that automatically runs “ellipse” for a range of different initial parameters, performing up to 200 fits per galaxy. We successfully fitted ellipses to 90% of the 1590 galaxies, while the 10% failure cases included mostly very disturbed systems where no centering could be performed and some extended low surface brightness systems. For all fitted galaxies, we inspected the image (Fig. 1a), the fitted ellipses overlaid on the images (Fig. 1b), and the radial profiles (Fig. 1c) of intensity, ellipticity (e), and position angle (P.A.) in order to confirm that the best fit is reliable. This inspection was aided by a visualization tool that we developed. We identify a bar as such if the fitted ellipses and radial profiles show the following characteristic bar signature (e.g., Wozniak et al. 1995) illustrated in Fig. 1. (i) The ellipticity (e) must rise to a *global* maximum e_{max} , which we require to be above 0.25, as well as above that of the outer disk, while the P.A. has a plateau (within $\pm 20^\circ$) along the bar. (ii) Beyond the bar end, as the bar-to-disk transition occurs, e must drop by ≥ 0.1 , while the P.A. usually changes by $\geq 10^\circ$. From the profiles, we identify e , P.A., and semi major axes a of both the bar and the outer disk. We quantify the bar strength using e_{max} , which correlates locally with other measures of bar strength, such as the gravitational bar torque (Laurikainen, Salo, & Rautiainen 2002).

The sample of 1430 galaxies with successful ellipse fits includes galaxies of different morphological types (disks and spheroids), inclinations, and absolute magnitudes. We apply two cuts at $M_V \leq -19.3$ and -20.6 . The first cut gives us a sizeable sample of galaxies with a range of absolute magnitudes (-19.3 to -23.8) similar to that of the Ohio State University (OSU) survey, which is used to define the local bar fraction (E02). However, K -corrections based on local Scd templates (Coleman, Wu, & Weedman 1980) suggest that we are only complete out to $z \sim 0.8$ for

¹³ We assume in this paper a flat cosmology with $\Omega_M = 1 - \Omega_\Lambda = 0.3$ and $H_0 = 70 \text{ km s}^{-1} \text{ Mpc}^{-1}$.

the first cut. The second more stringent cut at -20.6 ensures completeness out to $z \sim 1.0$, but it reduces the sample drastically (see Table 1). In addition, to ensure reliable bar detection, we use the disk inclination i from ellipse fits (§ 2.2) to exclude highly inclined ($i > 60^\circ$) galaxies.

The optical bar fraction f_{opt} is defined as $(N_{\text{bar}}/N_{\text{sp/disk}})$ where $N_{\text{sp/disk}}$ is the number of spiral or disk galaxies, and N_{bar} is the number of such systems hosting bars. We identify spiral/disk galaxies using three independent techniques (Table 1). We first use the criterion $n < 2.5$, where n is the index of single-component Sersic models fitted to GEMS galaxies (B. Häussler et al. 2004, in preparation) with the GALFIT (Peng et al. 2002) package. Our choice of $n < 2.5$ is dictated by the fact that a study of GEMS galaxies at $z \sim 0.7$ (Bell et al. 2004), as well as tests in which we insert artificial galaxies in the GEMS fields, suggest that a Sersic cut of $n \leq 2.5$ picks up disk-dominated systems. The second technique uses a cut $C < 3.4$, where C is the CAS (Conselice et al. 2000) concentration index. Third, we use rest-frame $U - V$ color cuts in the range 0.8–1.2 to broadly separate spiral galaxies from red E/S0s, based on local SED templates and the observed red sequence at $z \sim 0.7$ (Bell et al. 2004).

3. RESULTS AND DISCUSSION

The bars that we identify primarily have ellipticities $e \geq 0.4$ and semi major axes a in the range $0''.15$ – $2''.2$ and 1.2–13 kpc (Fig. 2). Our experiment of artificially red-shifting B -band images of a subset of OSU galaxies out to $z \sim 1$ shows that it is difficult to unambiguously identify weaker ($e \leq 0.3$) bars, and we limit the discussion in this Letter to strong ($e \geq 0.4$) bars. Table 1 shows the optical bar fraction f_{opt} of such bars in the two redshift slices ($0.25 < z \leq 0.70$ and $0.7 < z \leq 1.0$) derived in the reddest filter and in a relatively fixed rest-frame band (§ 2.2). Results for $M_V \leq -19.3$ are shown, based on 627 galaxies out of which we identify 258 moderately inclined ($i < 60^\circ$) spirals that host ~ 80 bars. The consistency in the six entries attests to the robustness of the results and shows that the fraction of optically visible bars remains in the range 23%–36% or at $\sim 30\% \pm 6\%$ in both slices. Incompleteness effects (§ 2.2) do not bias the results since the cut at -20.6 gives similar bar fractions, shown in brackets (Table 1). The bar fraction is slightly higher in the rest-frame I band than B band, possibly indicative of dust and star formation masking bars at bluer wavelengths. Our findings of a fairly constant f_{opt} are consistent with E04 and do not show the dramatic decline in f_{opt} reported by A99.

More than 40% of the bars that we detect have semi major axes $a < 0''.5$ (Fig. 2), and many of these smallest bars may have been missed in earlier WFPC2 (e.g., A99) and NICMOS studies that did not benefit from the small ($0''.05$) ACS pixels, and the resulting narrow PSF. In addition to the wider WFPC2 PSF, cosmic variance, low number statistics, and methodology may have led to the lower f_{opt} reported by A99, but we cannot address this issue further here as the coordinates of galaxies in that study have not been published.

How do our results compare to f_{opt} for correspondingly strong bars in the local universe? There are as yet no statistics published on $z \sim 0$ bars based on a large volume-limited sample such as the Sloan Digitized Sky Survey.

As the next best alternative, we turn to the OSU sample (E02). For $i < 60^\circ$ spirals, we find $f_{\text{opt}} \sim 37\%$ for strong bars classified according to the visual RC3 ‘SB’ bar class, and $f_{\text{opt}} \sim 33\%$ for strong bars classified according to $e \geq 0.4$, where e is based on ellipse fits to OSU B -band images. Thus, *it appears that the optical fraction of strong ($e \geq 0.4$) bars remains remarkably similar at $\sim 30\%$ – 37% from the present-day out to look-back times of 2–6 Gyr ($z \sim 0.2$ – 0.7) and 6–8 Gyr ($z \sim 0.7$ – 1.0).* Our findings have several implications for disk and bar evolution. (1) The abundance of strong bars at early times implies that dynamically cold disks that can form large-scale stellar bars are already in place by $z \sim 1$. They also suggest that highly triaxial, centrally concentrated DM halos, which tend to destabilize the bar (El-Zant & Shlosman 2002), may not be prevalent in galaxies at $z \sim 0$ –1. (3) The remarkably similar fraction of strong bars at look-back times of 6–8 Gyr, 2–6 Gyr, and in the present day supports the view that large-scale stellar bars are long-lived (e.g., Athanassoula 2002; Shen & Sellwood 2004; Martinez-Valpuesta et al. 2004), with a lifetime well above 2 Gyr. The alternative option, statistically allowed by the data, is that the combined destruction and reformation timescale of bars is on average well below 2 Gyr. However, this is highly implausible because the destruction of a bar leaves behind a dynamically hot disk that cannot reform a bar unless it is substantially cooled via processes that take at least several Gyr, such as the accretion of large amounts of cold gas. (3) We note that a similar *fraction* of bars at different epochs does not exclude the possibility that the bar strength (ellipticity) and its size can evolve in time because of intrinsic factors and concurrent changes in the surrounding disk, bulge and halo potentials (e.g., Athanassoula 2002; Martinez-Valpuesta & Shlosman 2004). Kolmogorov-Smirnov tests on the distributions of e and a for different magnitude cuts yield primarily P in the range 0.2–0.5, where P is the significance level for the null hypothesis that the two data sets are drawn from the same distribution. Such values of P hint at evolutionary effects, but a larger sample is needed to draw definite conclusions. While this Letter focuses on the optical bar *fraction*, in Paper II, we will invoke the full GEMS sample of 8300 galaxies to compare bar and host galaxy properties (e.g., disk scale lengths, masses, and B/D ratios) over the last 8 Gyr at 1 Gyr intervals.

S.J., F.D.B., I.S., and D.H.M. acknowledge support from NASA/LTSA/ATP grants NAG5-13063, NAG5-13102, and ATP 5-10823, and NSF AST02-06251. E.F.B. and S.F.S. acknowledge support from ECHPP under HPRN-CT-2002-00316, SISCO, and HPRN-CT-2002-00305, Euro3D RTN. C.W. was supported by a PPARC Advanced Fellowship. Support for GEMS was provided by NASA through GO-9500 from STScI, which is operated by AURA, Inc., for NASA, under NAS5-26555.

REFERENCES

- Abraham, R. G., Merrifield, M. R., Ellis, R. S., Tanvir, N. R., & Brinchmann, J. 1999, MNRAS, 308, 569 (A99)
- Athanassoula, E. 2002, ApJL, 569, L83
- Bell, E. F., et al. 2004, ApJL, 600, L11
- Benítez, N., et al. 2004, ApJS, 150, 1
- Bournaud, F. & Combes, F. 2002, A&A, 392, 83
- Coleman, G. D., Wu, C.-C., Weedman, D. W. 1980, ApJS, 43, 393
- Conselice, C. J., Bershad, M. A., & Jangren, A. 2000, ApJ, 529, 886
- Elmegreen, B. G., Elmegreen, D. M., & Hirst, A. C. 2004, ApJ, accepted (E04)
- Eskridge, P. B., et al. 2002, ApJS, 143, 73 (E02)
- El-Zant, A. & Shlosman, I. 2002, ApJ, 577, 626
- Friedli, D. & Benz, W. 1993, A&A, 268, 65
- Hunt, L. K. & Malkan, M. A. 1999, ApJ, 516, 660
- Jogee, S., Kenney, J. D. P., & Smith, B. J. 1999, ApJ, 526, 665
- Jogee, S., Knapen, J. H., Laine, S., et al. 2002, ApJL, 570, L55
- Jogee, S., Scoville, N. Z., & Kenney, J. 2004a, ApJ, submitted (astro-ph/0402341)
- Jogee, S., Barazza, F., Rix, H.-W., et al. 2004b, in Penetrating Bars through Masks of Cosmic Dust, eds. D. Block, K. Freeman, R. Groess, I. Puerari, & E.K. Block (Dordrecht: Kluwer), in press (astro-ph/0408267)
- Knapen, J. H., Shlosman, I., & Peletier, R. F. 2000, ApJ, 529, 93
- Kormendy, J. & Kennicutt, R. C. 2004, ARAA, 42, 603
- Kormendy 1982, in Morphology and Dynamics of Galaxies, Twelfth Advanced Course of the Swiss Society of Astronomy and Astrophysics, eds. L. Martinet and M. Mayor, 113
- Laurikainen, E., Salo, H., & Rautiainen, P. 2002, MNRAS, 331, 880
- Martinez-Valpuesta, I., Shlosman, I. & Heller, C.H. 2004, ApJ, submitted
- Martinez-Valpuesta, I. & Shlosman, I. 2004, ApJL, 613, L29
- Peng, C. Y., Ho, L. C., Impey, C. D., & Rix, H. 2002, AJ, 124, 266
- Pfenniger, D. & Norman, C. 1990, ApJ, 363, 391
- Regan, M. W., Vogel, S. N., & Teuben, P. J. 1997, ApJL, 482, L143
- Rix, H., et al. 2004, ApJS, 152, 163
- Sakamoto, K., et al. 1999, ApJ, 525, 691
- Shen, J. & Sellwood, J. A. 2004, ApJ, 604, 614
- Sheth, K., Regan, M. W., Scoville, N. Z., & Strubbe, L. E. 2003, ApJL, 592, L13 (S03)
- Shlosman, I., Frank, J., & Begelman, M. C. 1989, Nature, 338, 45
- Shlosman, I. & Noguchi, M. 1993, ApJ, 414, 474
- Wolf, C., et al. 2004, A&A, 421, 913
- Wozniak, H., et al. 1995, A&A Suppl., 111, 115

TABLE 1
OPTICAL FRACTION f_{opt} OF STRONG ($e \geq 0.4$) BARS AT
 $0.25 < z \leq 0.70$ ($T_{\text{back}} \sim 2\text{--}6$ GYR) AND $0.7 < z \leq 1.0$ ($T_{\text{back}} \sim 6\text{--}8$ GYR)

| Redshift range | N_{gal} | Technique to identify disks/spirals | $N_{\text{sp/disk}}$ | Filter to trace bars | Rest-frame band | Optical bar fraction f_{opt} |
|--|------------------|-------------------------------------|----------------------|----------------------|-----------------|---------------------------------------|
| (1) | (2) | (3) | (4) | (5) | (6) | (7) |
| Method I: Using the reddest ACS filter (F850LP) to identify bars | | | | | | |
| 0.25–0.70 | 384 (146) | Sersic n | 148 (39) | F850LP | I to V | 36% (33%) |
| 0.70–1.0 | 243 (135) | Sersic n | 110 (49) | F850LP | V to B | 24% (27%) |
| 0.25–0.70 | 384 (146) | CAS C | 170 (51) | F850LP | I to V | 27% (27%) |
| 0.70–1.0 | 243 (135) | CAS C | 147 (73) | F850LP | V to B | 23% (23%) |
| 0.25–0.70 | 384 (146) | $U - V$ | 175 (51) | F850LP | I to V | 29% (28%) |
| 0.70–1.0 | 243 (135) | $U - V$ | 139 (69) | F850LP | V to B | 29% (26%) |
| Method II: Using F606W and F850LP to identify bars at an approximately fixed rest-frame B/V band | | | | | | |
| 0.25–0.70 | 384 (146) | Sersic n | 148 (39) | F606W | V to B | 26% (30%) |
| 0.70–1.0 | 243 (135) | Sersic n | 110 (49) | F850LP | V to B | 24% (27%) |
| 0.25–0.70 | 384 (146) | CAS C | 170 (51) | F606W | V to B | 24% (28%) |
| 0.70–1.0 | 243 (135) | CAS C | 147 (73) | F850LP | V to B | 23% (23%) |
| 0.25–0.70 | 384 (146) | $U - V$ | 175 (51) | F606W | V to B | 29% (23%) |
| 0.70–1.0 | 243 (135) | $U - V$ | 139 (69) | F850LP | V to B | 29% (26%) |

Note. — Col. (1): The redshift range. Col. (2): The no of galaxies in this range with $M_V \leq -19.3$ and -20.6 (shown in brackets) to which ellipses were fitted. Col. (3): The technique used to identify disk/spiral galaxies from the sample in (2). We use cuts of Sersic index $n < 2.5$, CAS concentration index $C < 3.4$, and rest-frame $U - V < 0.8\text{--}1.2$. Col. (4): $N_{\text{sp/disk}}$, the no of moderately inclined ($i < 60^\circ$) spiral/disk galaxies for the two magnitude cuts in (2). Col. (5),(6): The filter and rest-frame band in which bars are traced; Col. (7): f_{opt} , the optical fraction of strong bars, is the fraction ($N_{\text{bar}}/N_{\text{sp/disk}}$) of moderately inclined spirals hosting bars with $e \geq 0.4$. Values for the two magnitude cuts of -19.3 and -20.6 are shown.

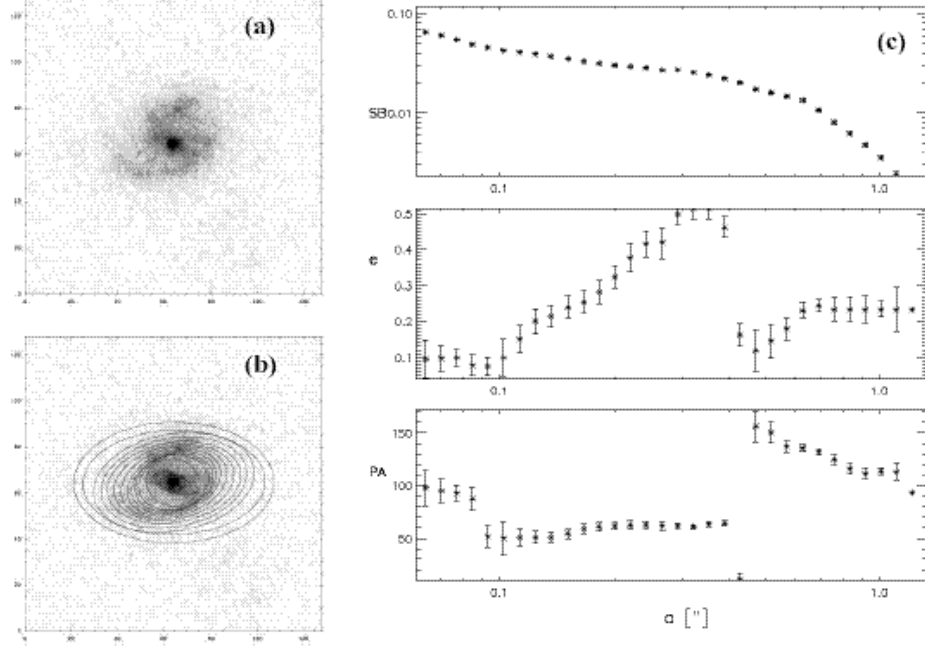


FIG. 1.— Characterization of bars out to $z \sim 1.0$: The GEMS image of a $z \sim 0.5$ galaxy with a bar, prominent spiral arms, and a disk is shown without (a) and with (b) an overlay of the fitted ellipses. (c) In the resulting radial plots of the surface brightness, ellipticity e , and P.A., the bar causes e to rise smoothly to a global maximum, while the P.A. has a plateau. Beyond the bar end ($a \sim 0''.36$), the spiral arms lead to a twist in P.A. and varying e before the disk dominates.

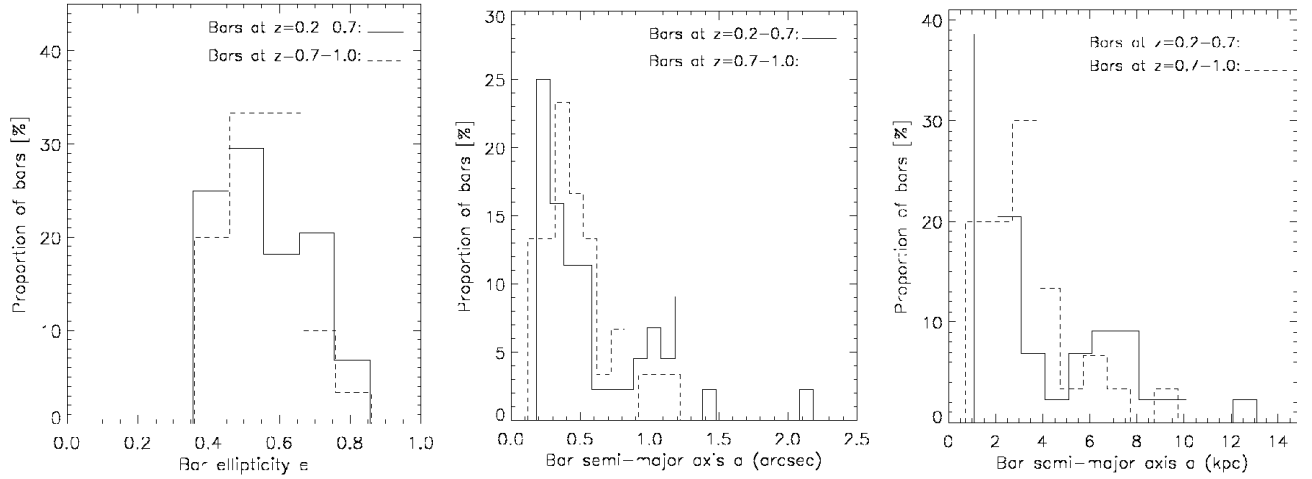


FIG. 2.— Comparison of bars out to look-back times of 8 Gyr: The bar ellipticity e (left) and semi major axis a in '' (middle) and kpc (right) are shown for bright ($M_V \leq -19.3$), moderately inclined ($i < 60^\circ$) galaxies at $z \sim 0.2-0.7$ ($T_{\text{back}} \sim 2-6$ Gyr) and $z \sim 0.7-1.0$ ($T_{\text{back}} \sim 6-8$ Gyr). The bars identified are primarily strong, with $e \geq 0.4$. A large fraction have $a < 0''.5$ and their detection is aided by the narrow ACS PSF.